# A theorist in industry

Helvetica Physica Acta,
Vol. 56 (1983) 349-359

0018-0238/83/010349-11$1.50+0.20/0


# A THEORIST IN INDUSTRY

G.J. Rees

Plessey Research (Caswell) Limited
Allen Clark Research Centre
Caswell, Towcester, Northants, U.K.

## ABSTRACT

The role of Theoretical Technologist is discussed and commended, with some illustrative examples.

## INTRODUCTION

Theoretical Physicists working in the electronics industry are usually known to their university counterparts for the work which they publish at conferences and in journals on physics. In some industrial laboratories this work indeed represents a major part of their day to day activities. In other organizations, including Plessey-Caswell, theoreticians are additionally encouraged to become involved with the more immediate problems facing device technologists. Consequently they find themselves drawn into performing calculations whose results can change the direction of practical device research in the short term, as well as the long term. Close collaboration between theorist and technologist is not always easy; a common language has to be learnt, usually by the theorist. However the immediacy of impact is invariably rewarding and such collaboration can be fruitful. The role of theoretical technologist fills an important gap in the spectrum of disciplines in many industrial laboratories and perhaps university departments.

At Plessey-Caswell a small group of theorists and mathematicians operate among a large number of scientists and technologists engaged in practical materials and device research and development. The ratio ensures a constant stream of problems from which we can choose those which are important, interesting and solvable. In an attempt to give you some insight into our mainstream activities I shall describe a few such problems. My choice is biassed towards shorter and more immediately accessible topics which can be described in half an hour. I have chosen them from the fields of microwave engineering and optoelectronics.

## 1. MIXING IN NONLINEAR DEVICES

The response of a nonlinear device to harmonic signals has been appreciated since the days of crystal sets and cats' whiskers.

When a voltage signal

$$V(t) = V_1\cos(\omega_1 t) + V_2\cos(\omega_2 t) \quad (1)$$

varying in time as the sum of two harmonic components of angular frequency $\omega_1$ and $\omega_2$, is applied to a non linear current-voltage characteristic I(V) then the resultant current can be expressed as a harmonic series:

$$I(V(t)) = \sum I_{m,n}(V_1,V_2)\cos(m\omega_1 + n\omega_2)t \quad (2)$$
$$(m \text{ and } n \text{ are } (\pm)\text{ve integers})$$

with components whose frequencies are integral multiples of $\omega_1$ and $\omega_2$. This can most easily be seen by expanding the I(V) curve as a power series:

$$I(V) = a + bV + cV^2 + dV^3 + eV^4... \quad (3)$$

substituting for V(t),simplifying with multiple angle formulae and regrouping.

Thus the "Intermodulation Product" (IP) $I_{m,n}(V_1,V_2)$ corresponding to (m,n) = (1, -1), known as the "Intermediate frequency" (IF) has the form:

$$I_{1,-1}\ (V_1,V_2) = cV_1\ V_2/2 + 3e(V_1^3\ V_2 + V_1\ V_2^3)/2 + \ldots$$

Whilst the principle contribution comes from the quadratic term in equation (3) all even order terms in the series contribute.

One application of this frequency mixing effect is in satellite TV (Figure 1). A ground station transmits a TV signal at a radio frequency $\omega_{RF}$, up to a geostationary satellite. This signal is mixed in the satellite with a local oscillator of frequency $\omega_{LO}$ and the IF of frequency $\omega_{IF} = \omega_{RF} - \omega_{LO}$, is amplified and broadcast over a wide range to ground stations or domestic receivers. The frequency down conversion avoids saturating the receiver on the satellite with the rebroadcast signal. In addition to the IF the mixer also produces the full spectrum of IPs at frequencies $m\omega_{RF}+n\omega_{LO}$ which the ground receiver station, tuned to the IF, does not see. However the satellite is used to rebroadcast, on the same principle, RF signals from a variety of ground transmitters at a variety of frequencies. An IP formed from one RF signal may interfere with the IF formed from another. We there-

fore need a way of predicting IP levels from the non linear I(V)characteristic of our mixer - in our case the source-drain current vs gate voltage of a GaAs FET. Our prediction would then enable us to choose, or modify our device to minimise these higher order IPs.

There are two standard ways of calculating mixing effects: One is as described and involves power series expansion of the nonlinearity and recollection of the terms calculated from multiple angle formulae. This procedure requires very high order terms in the power series to secure convergence, reflecting the high order IPs involved. The procedure is tedious, inaccurate and unreliable for large signal levels. The alternative is to simulate the current wave form (equation 2) and numerically Fourier analyse the result into its spectral components. The total elapsed time of the truncated signal will increase as the inverse of the lowest frequency IP under study whilst the number of time steps is determined by the high frequency spectral components. This technique is also inaccurate, expensive of computing time and clumsy.As an alternative to these conventional methods we note that the information we seek, namely the form of $I_{m,n}(V_1,V_2)$ is independent of $\omega_1$, $\omega_2$ and t. We are at liberty therefore to average over frequency or time without destroying the key information. Using this technique [1] we arrive at a simple formula for IP levels:

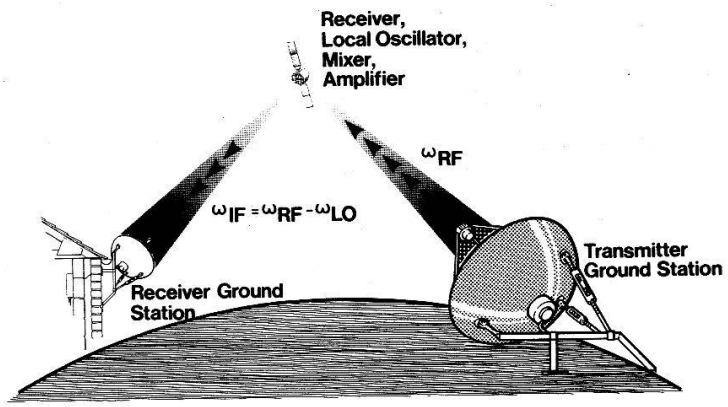


Fig.1: Satellite TV

$$I_{m,n}(V_1,V_2) = \frac{1}{2\pi^2}\int_0^{2\pi}\int_0^{2\pi} d\theta\, d\phi \cos(m\theta+n\phi) I(V_1\cos\theta+V_2\cos\phi) \qquad (4)$$

(divide RHS by 2 for m = o = n). With hindsight this results becomes obvious if we make the substitution $\omega_1 t = \theta$, $\omega_2 t = \phi$ in equation (2):

$$I(V_1\cos\theta+V_2\cos\phi) = \sum I_{m,n}(V_1,V_2)\cos(m\theta+n\phi) \qquad (5)$$

which we recognise as a 2-D Fourier series of which equation (4) is the inverse.

Armed with this simple result we can now evaluate IPs with arbitary order and accuracy by numerically performing a double integral. The I(V) curve is only needed over the range of voltages accessed by the signals and there is no constraint on the range of frequencies studied.

Figure 2 shows calculations of IP power level for a range of IPs (m,n) as a function of DC gate bias voltage. The corresponding I(V) curve is shown in the inset.

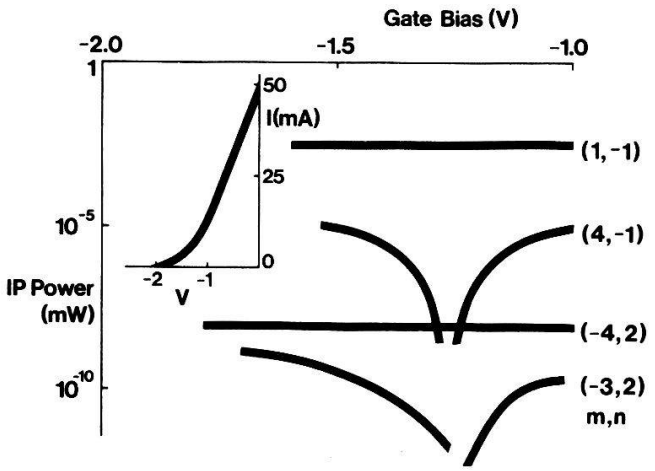


Fig.2: IP power levels and I(V) (inset)

The IF (1,-1) is seen to be substantially flat but the IPs (4,-1) and (-3,2) change bias at around -1.2 volts. This result is particularly useful since the IP (4,-1) cannot be otherwise eliminated by simple balancing techniques in the satellite mixer.

The zeroing of certain IPs can be shown to

arise from a hidden near symmetry in the I(V) curve which becomes obvious on differentiating. The result follows in a straightforward manner from the closed form expression in equation (4).

In practice the FET cannot accurately be represented by a simple, instantaneous I(V) curve and its equivalent circuit contains in addition nonlinear capacitors and inductors. IP currents generate IP voltages flowing through linear elements and as a result we need to generalise equation (4) to allow for the possibility that all orders of IP in voltage will appear across a nonlinear element. In fact if the voltage wave form is

$$V(t) = \sum V^{c}_{p,q} \cos\,(p\omega_1+q\omega_2)t + V^{s}_{p,q} \sin(p\omega_1+q\omega_2)t$$

then the corresponding current through a nonlinear element I(V) is given by

$$I(V(t)) = \sum I^{c}_{m,n} \cos(m\omega_1+n\omega_2)t + I^{s}_{m,n}\sin(m\omega_1,+n\omega_2)t$$

where

$$I^{c,s}_{m,n} = \frac{1}{2\pi^2} \int_0^{2\pi}\!\!\int_0^{2\pi} d\theta\, d\phi \begin{matrix}\cos\\ \sin\end{matrix}(m\theta+n\phi)\, I\Big(\sum V^{c,s}_{p,q} \begin{matrix}\cos\\ \sin\end{matrix}(p\theta+q\phi)\Big)$$

(divide RHS by 2 for m = 0 = n).

This procedure offers a new, faster way of evaluating the spectral response of nonlinear systems with memory and has numerous applications in radar, heterodyning and distortion analysis of nominally linear circuits.

## 2. OPTICAL SATURATION IN FACE EMITTING LEDs

The face emitting LED (Figure 3) is widely used to launch power into optical fibres. The active part of the device is the central, shaded disc of quaternary alloy semiconductor, GaInAsP, chosen for its band gap and optical emission spectrum matched to the transmission characteristics of the fibre. On either side are layers of wider band gap InP and these serve both to inject and confine carriers in the active region under forward bias. Recombination of injected carriers produces radiation which escapes through the wide gap cladding layers via the lens into the fibre.

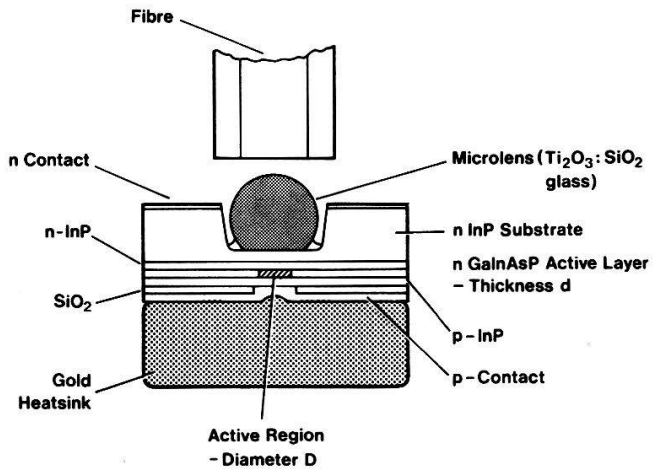


Fig.3: Face emitting LED

The principles of operation of these double heterostructure spontaneous emitters are well known but they have the disadvantage that the optical output saturates at high current levels (Figure 4) and this effect was the subject of our investigation. There were three principle contenders for an explanation, which are discussed in turn.

## 2.1. INCOMPLETE CARRIER CONFINEMENT

At high currents the carrier concentration builds up in the active layer, the quasi-Fermi level rises and it becomes easier for carriers to jump the potential barrier and become minority carriers in the adjacent InP layer, escaping to recombine unproductively elsewhere. This loss will increase with current level and lead to saturation of the optical output. However thermal activation over the barrier should be strongly temperature dependent, contrary to observations.

## 2.2 AUGER RECOMBINATION

In the lightly doped active region the injected electron and hole concentrations are equal, $n = p$, and the radiative recombination rate is proportional to $n^2$. On the other hand Auger recombination involves three carriers and its rate is proportional to $n^3$. The current I feeds both of these processes: $I = Bn^2 + Cn^3$ and at high injection levels, when Auger recombination dominates the current, the optical output, $L = Bn^2$, should depend sublinearly on current as $L \alpha J^{2/3}$. This asymptotic behaviour runs parallel to the "Auger" line in figure 4 and the sublinearity is insufficiently saturating to account for the observations.

## 2.3 IN-PLANE SUPERLUMINESCENCE

In fact we believe the clue to radiance saturation lies in the high current densities, many times solid state laser threshold, and the lateral optical confinement produced by the reduced refractive index of the wider gap, cladding InP.

In addition to the spontaneous radiation emitted through the front face photons are preferentially guided sideways. In the inverted population of the high injected carrier concentrations recombination is stimulated, producing further laterally guided photons. Because of the high aspect ratio of the disk, around 2 microns thick by tens of microns in diameter, lateral stimulated emission is a strong process and is unproductive since lateral light is absorbed in the unpumped regions beyond the disk edge. Thus at high injection levels the carriers, intended to produce forward directed spontaneous radiation into the fibre,are preferentially stimulated to recombine,producing useless, sideways travelling light.

A simple model [2] sufficed to test the strength of this effect. Given the refractive indices, $n_c$ and $n_g$ of the cladding and guiding regions

we can calculate the fraction, $f = (1-(n_c/n_g)^2))^{\frac{1}{2}}$ of spontaneously generated light waveguided between the cladding layers. Assuming a spontaneous radiative recombination lifetime, $\tau$ and a uniform carrier concentration in the active region the light emitted spontaneously from both faces of the active disk, of diameter D and thickness t is

$$L_F = \pi n t D^2 (1-f)/4\tau.$$

As for the light emitted from the disk edge we have to consider spontaneous emission generated within an elementary volume in the disk and its amplification by uniform gain, g, all the way out to the disk edge. The result of integrating the light emerging from around the perimeter and summing these contributions originating from all over the disk is that the edge emitted light is given by

$$L_E = tDf\pi n(L_1(-gD) - I_1(-gD))/2\tau g$$

where $I_1$ and $L_1$, are modified Bessel and Struve functions. Ignoring any nonradiative recombination the current needed to feed this optical output is

$$I = e(L_E + L_F)$$

where e is the electronic charge.

Figure (4) shows front face optical output as a function of current density for devices of various diameter. The absolute magnitude of output is over-estimated, perhaps because of neglect of nonradiative recombination. However the degree of saturation and its dependence on device diameter are adequately explained considering the simplicity of the model.

Following this understanding ingenious mechanisms [3] were devised using 45° preferential etches to produce integrated retroreflectors redirecting this lateral light towards the front face. This laterally directed high optical power is used to advantage in superluminescent edge emitting LEDs whose small emitting surface areas are better suited to modern, single mode optical fibres.

## 3. SUPERLUMINESCENT, EDGE EMITTING LED

This device, which has been around for some time, is shown schematically in figure 5. The active region is still narrow gap quaternary InGaAsP, clad with InP to afford optical and carrier confinement. But now the active region is in the form of a rectangular block, say of width W = 15 μm, length L = 150 μm and thickness 0.2 μm. The width is defined by proton implanting the surround or by confining the current to restrict the injected carriers. The optically emitting end face is cleaved and the dielectric mismatch with

air produces a Fresnel reflectivity R = 0.3. The other end of the pumped, active region is buried in the layer so that light travelling backwards is lost. This device offers higher radiance than a face emitting LED and faster response due to the stimulated recombination but is not as temperamental as a solid state laser. It has been studied for sometime at various laboratories but the many degrees of design freedom including geometry, facet reflectivity (anti-reflection coating), doping level and option of lateral guiding from buried heterostructure provide a bewildering set of options which affect spectral response, speed, power output and temperature dependence. As a guide to optimisation a device model is required for rapid evaluation. Models exist in the literature

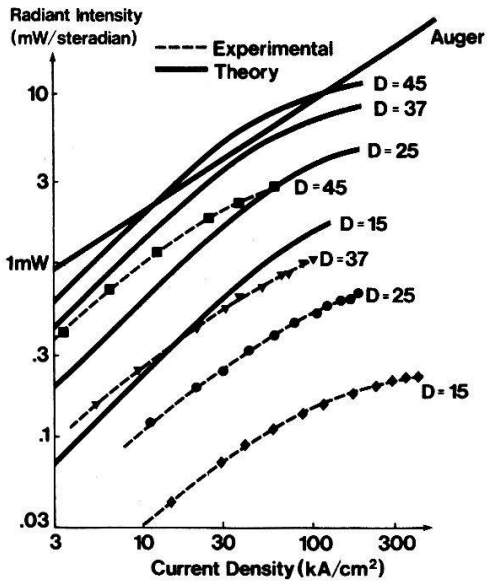


Fig.4: Light vs current showing saturation

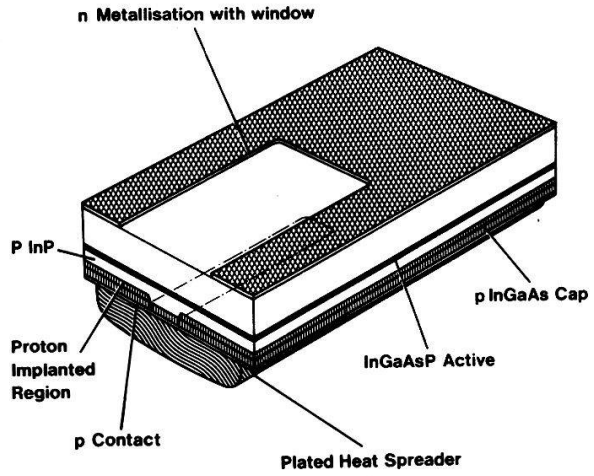


Fig.5: Edge Emitting LED

[4] but they are either prohibitively time consuming to operate or inadequately simple.

Our approach in devising a model followed the lines of the simple calculation on front face emitters, but with a few more refinements since we are concerned with the detailed behaviour of the device and not merely one pathological aspect. We assume a uniform carrier distribution within the active layer and calculate the optical outputs from the various faces, allowing for both gain and internal loss. We also make allowance for nonradiative recombination. The thickness, t of the active region is small so in this direction a wave description of the optical field is necessary. We must therefore scale down the gain by the optical confinement factor and also make allowance for modal refractive index (in a ray picture this would correspond to the increased path length of zig-zag rays). In the lateral direction we assume no optical guiding and since the width, W and length, L are large compared with wavelength a ray picture suffices.

Calculating optical output, say from the cleaved end face, involves summing the spontaneous contributions from the complete emitting area WxL of the active region and also integrating over the direction of the emitted light, allowing for the exponential amplification as the light passes through the inverted carrier population. The resulting triple integral can, by juggling with the order of integration, be reduced to a single integral which presents no problems numerically. Emission from the sides and rear face present precisely the same geometrical problem which is therefore solved.

The light Fresnel reflected from the front face is a bit more difficult since on reflection it enjoys gain in the active region and emerges elsewhere. In fact this contribution can be handled by an "image active region" which is just the real active region reflected in the cleaved facet. The contribution of this source can be linearly related to simple geometrical contributions which are just scalings of those already calculated, so that problem is solved, too. Finally, we must calculate the light lost by irreversible absorption within the active region. For a ray propagating in a uniform medium this is easily shown to be $\alpha(L(g)-L(0))/g$ where $L(g)$ is the optical power emitted for a net gain $g$ and $\alpha$ is the gross loss. This result can also be shown to hold for our entire device.

It merely remains to choose material and optoelectronic parameters [5] such as the dependence of gain on injected carrier level, and turn the

handle. Sample results of this process are shown in Figure 6, predicting optical output, modulation bandwidth and peak emission wavelength as a function of drive current. This work is still in its early stages and the model will be refined by comparison with measurement and more judicious choice of material parameters.

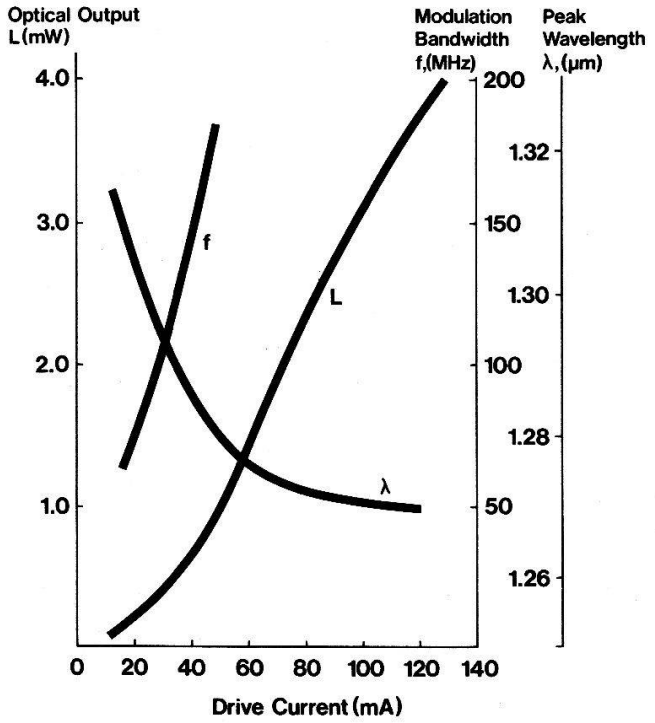


Fig.6: Model results for EELED

## 4. CONCLUSIONS

Theoretical physicists have a more immediate role in the electronics industry than that of performing long range research. The gap which so often exists between theorist and technologist is too wide not to bridge and if he so chooses the theorist can turn his analytical talents on a whole new range of rewarding and useful problems.

## REFERENCES

[1] Rees, G.J.; IEE Proc., 129H, 188 (1982)

[2] Goodfellow, R.C., Carter, A.C., Rees, G.J. and Davis, R; IEE Trans ED-28,365 (1981).

[3] Carter, A.C., Goodfellow, R.C. and Griffith, I; Proc. IEDM, Washington, 118, (1979).

[4] Marcuse, D., IEEE J. QE-17, 1234 (1981) and references therein.

[5] Osinski, M. and Adams, M.J., IEE Proc., 129H, 229 (1982).